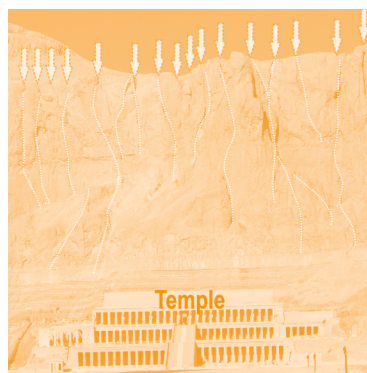


Geological appraisal of the Theban cliff overhanging the Hatshepsut temple at Deir el-Bahari



Abstract: Throughout its existence the Temple of Hatshepsut, as well as two other royal sanctuaries, the temples of Mentuhotep II and Thutmose III, located in the great bay of Deir el-Bahari, have been under constant threat of falling rocks from the overhanging Theban cliff. The PCMA UW archaeological expedition at Deir el-Bahari, which has progressed with the study and conservation of the Hatshepsut temple since the 1960s, has implemented a project designed to address the issue of the protection of the temple from damages that could be caused by environmental processes (rainwater and seismic activity) affecting the Theban cliff behind the monument. In a geological survey of the fractured limestone cliff, the evidence from 31 observation stations was appraised and samples of Esna Shale and Theban Limestone were examined in order to ascertain the degree of the cliff's instability and fragility. The results were used to prepare a 2D model presenting the environmental processes threatening the ancient substance.

Keywords: Theban Limestone cliff, Esna Shale, Temple of Hatshepsut, Deir el-Bahari, geological research, swelling rate

The rocky circus of Deir el-Bahari is part of the Theban Necropolis on the western bank of the Nile, facing Luxor in Upper Egypt. In the 15th century BCE, the Eighteenth-Dynasty female-pharaoh Hatshepsut

Patryk Chudzik¹
Ahmed-Reda M. El Younsy²
Wael F. Galal³
Abdelhamid M. Salman⁴

¹ Polish Centre of Mediterranean Archaeology, University of Warsaw
^{2,3,4} University of Asyut, Faculty of Science, Geology Department

Acknowledgments

The authors express their gratitude to the Director and staff of the Polish Centre of Mediterranean Archaeology, University of Warsaw, for financial support and invaluable assistance throughout the season. Words of appreciation also go to the authorities of the Egyptian Ministry of Tourism and Antiquities, both in Cairo and Luxor, for their friendly cooperation, understanding and support on all matters related to the fieldwork. Thanks are also addressed to the Supreme Council of Antiquities, represented by Mr. Khalid El Taib Mohamed, inspector of antiquities in the region, for his efforts and guidance during the fieldwork. Special thanks to the inspector Mr. Ayman Amer for placing the research team from Asyut in contact with the PCMA UW expedition in Deir el-Bahari (Luxor).

chose this bay for her ‘House of Millions of Years’, an extraordinary mortuary temple called *Djeser-djeseru* (‘Holy of Holies’). The terraced temple was partly cut into the Esna Shale formation, sandwiched between two limestone rock units: the highly fractured Theban Limestone above and the buried Tarawan Chalk below. Throughout its existence, the building has been endangered by rockfalls and natural processes taking place in the rock. The Polish Centre of Mediterranean Archaeology, University of Warsaw (PCMA UW) archaeological expedition to Deir el-Bahari, which has been engaged in the study and conservation of the temple since the 1960s, recognizes the potential hazards and has initiated

a comprehensive project for the protection of the ancient monuments from the effects of rainfall and seismic activity, extending the scope of the expedition’s work to the temple surroundings.

The issue has already been explored on a number of occasions (Said 1990; Dupuis et al. 2011; King et al. 2017), establishing the grounds for the current work, the aim of which is a new appraisal of the fractured Theban Limestone cliff behind the temple in terms of its fragility and the stability of the limestone ‘chimneys’ overhanging the temple area. A risk assessment of the location of the temples in the Deir el-Bahari circus was the outcome of the work carried out in 2020 and presented in this report.

HISTORICAL OVERVIEW

The first to build a mortuary temple in the rocky bay of Deir el-Bahari was Nebhepetra Mentuhotep II, a pharaoh from the Eleventh Dynasty, who reunited the country after a long period of political destabilization and a civil war (known in history as the First Intermediate Period) at the close of the 3rd millennium BCE. The bay was also a cult place of the cow-goddess Hathor, a patroness of the Theban necropolis, its roots in this area going back probably to the Old Kingdom (Bernhauer 1998: 15ff.; Niwiński 2008). Mentuhotep’s temple was situated on the southern side of Deir el-Bahari, directly opposite the Karnak Temple complex on the other bank of the Nile [Fig. 1]. Nearly five centuries later Djeserkara Amenhotep I, the second king of the Eighteenth Dynasty, chose the vast courtyard of this temple for a small enigmatic struc-

ture, built of mud bricks stamped with the names of the king and his mother, Ahmose-Nefertari (Dodson 1989–1990; Madej 2018) [see Fig. 1]. The remains of this building, presumably a shrine, were discovered by Herbert E. Winlock on the Middle Terrace of the Hatshepsut Temple, north of the Lower Ramp (Winlock 1924: 14–16; 1928a: 28, 30, Fig. 26). It had been demolished by workmen building Hatshepsut’s ‘House of Millions of Years’.

The most famous and magnificent royal monument at Deir el-Bahari, the Temple of Hatshepsut, occupies the northern part of the natural rocky bay formed by river and wind erosion. Modelled on Old Kingdom royal pyramid temples, the building took advantage of a vast ‘natural pyramid’, the Theban gebel, as a backdrop, the El-Qurn at the top of the mountain acting as a natural

pyramidion (Ćwiek 2014: 67–69; 2020; Ejsmond 2018: 174–176). The overall design of the complex, which was built by the accomplished Senenmut, overseer of the pharaohs' works, invoked the Old Kingdom 'classical' pyramid complexes: a Valley Temple at the edge of the cultivated area, a processional avenue lined by large sphinxes with heads of Hatshepsut (Winlock 1928b: 17–18; 1932: 10–14, Fig. 5; Smilgin 2012) and the Upper Temple at Deir el-Bahari (see Ćwiek 2014).

The Temple itself consists of a courtyard enclosed by a stone wall, and two higher terraces adjoining the rock cliff, reached by separate ramps. Pillared porticoes flanked the ramps on each level, and

an additional, third portico extended on either side of the monumental granite portal on the highest platform. The architectural design was directly inspired by the nearby mortuary temple of Mentuhotep II as well as by the pillared front porticoes of the rock-cut tombs of the early-Eleventh-Dynasty rulers bearing all the same name Intef, located at the nearby locality of el-Tarif (Arnold 2005: 135–136; Ćwiek 2014).

A rocky platform south of Hatshepsut's Temple, overlooking the older monuments, was chosen by the great pharaoh and warrior Thutmose III for his *Djeser-Akhet* ('Holy of Horizon') temple (Lipińska 1977; 2005) [see Fig. 1]. The

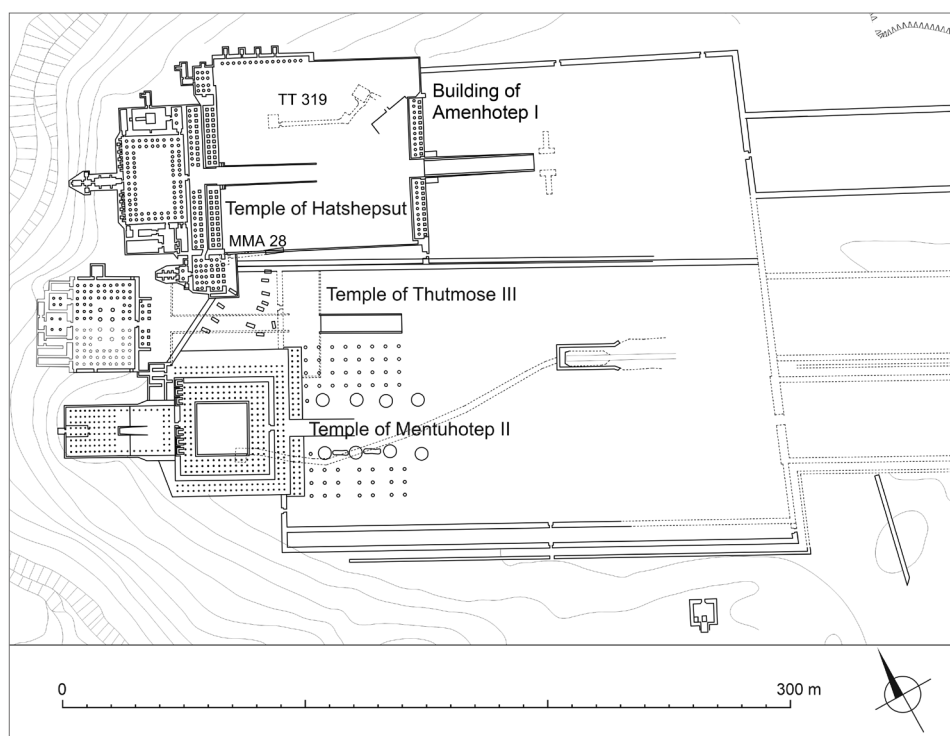


Fig. 1. Plan of the royal temples at Deir el-Bahari (PCMA UW | drawing K. Andraka, after Arnold 1979: Pl. 38 and Eigner 1984: Plan 1).

Temple was built in the last decade of the king's reign, apparently meant to overshadow Hatshepsut's sanctuary and to take over the principal role in the Beautiful Feast of the Valley, one of the main festivals of ancient Thebes. An earthquake, probably at the beginning of the Third Intermediate Period, destroyed the Temple of Thutmose III, covering it with hundreds of tons of rock debris.

A Coptic monastery dedicated to St Phoibammon was established in the ruins of the Hatshepsut temple at the end of

the 6th century CE, giving the site its Arab denomination, Deir el-Bahari ('Northern Monastery') (Godlewski 1986). The monastic complex was abandoned 200 hundreds years later, but continued as a Christian pilgrimage site until the early 13th century CE.

The royal monuments of Deir el-Bahari lay hidden under the rock debris until their discovery by archaeologists, which opened the way to the current extended research, restoration and conservation work in the area.

METHODOLOGY

Field mapping, collection of rock samples and exploration of the situation took place at 31 observation stations spread over three sectors (northeastern, southwestern, and the ground between these two) in Deir el-Bahari and the surrounding area.

A digital topographic map of the region comes from Landsat-8 OLI imagery issued by the U.S. Geological Service (<http://eros.usgs.gov>). The ALOS PAL-SAR Digital Elevation Model (DEM) was obtained from the Alaska Satellite Facility (2015).

The collected samples were analyzed to determine a rock and mineral characteristic and to estimate the clay mineral content. An X-ray Diffraction analysis

(XRD) was conducted at Asyut University on a Philips goniometer, using Ni-filtered CuK α radiation. Laboratory tests of selected samples at the Sedimentological Lab, Department of Geology, Asyut University, determined the free swelling rate.

Climatic data was obtained for the 1943 to 2020 interval to show the impact on the Deir el-Bahari region (sources: climatetoolbox.org; climatologylab.org). Historical photographs of the exposed, overhanging rock masses above the temple, the earliest coming from 1895, were also collected.

The results of these analyses were used to prepare a hypothetical impact model for the temple site.

GEOLOGICAL FRAMEWORK

TOPOGRAPHY

Three main geomorphological units are distinguished at Deir el-Bahari: limestone cliff, plain, and isolated hills. The cliff surrounds the temple area from

the northeast and extends irregularly southwest [Fig. 2:A–B]. It ranges in elevation between 200 and 140 m asl, reaching 240 m asl above the Temple. The top of the scarp extends monotonously

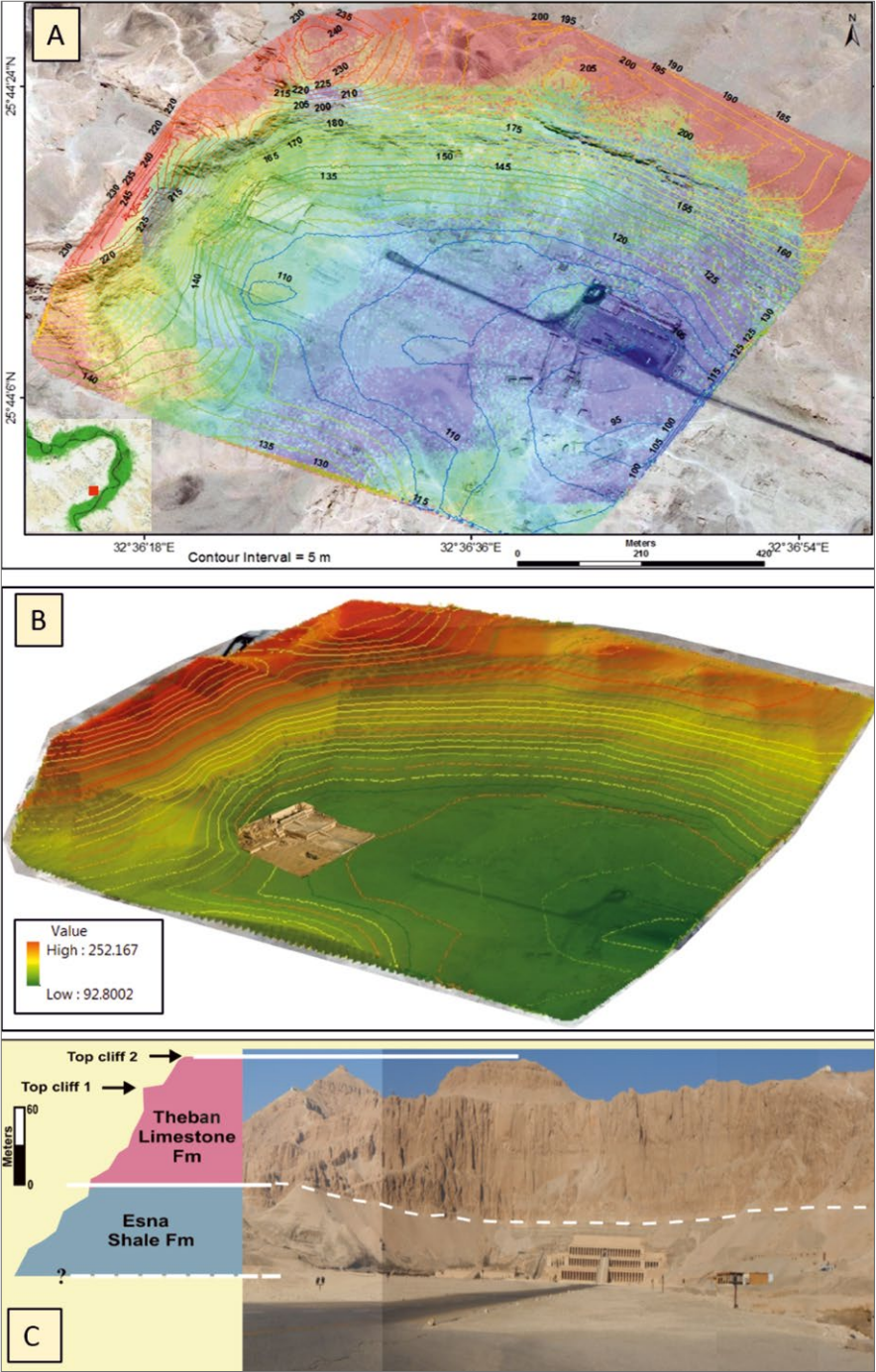


Fig. 2. The Deir el-Bahari circus: A – contour-line map based on Landsat-8 OLI images; B – 3D model using GIS; C – lithological units around the site with indication of sample positions (A, B, C – Esna Shale; D – Theban Limestone) (© Authors)

onously westward to the Valley of the Kings, displaying various karst features due to repeated dissolution effects caused by rain weathering in the past. The fracture systems of various trends and directions could increase this effect. The plain extends from the Nile Valley in the east to the Temple entrance, covering a vast semi-flat area varying in elevation from 95 to 135 m asl. Conspicuous isolated hills occur to the south of the entrance road to the Temple, with diverse landforms such as the el-Asasif (95 m asl) and Sheikh Abd el-Qurna (150 m asl) hills.

STRATIGRAPHY

Deir el-Bahari and the surrounding area are made up of sedimentary rocks composed principally of three geological rock units. These are, starting from the base: Tarawan Chalk of Paleocene age, Esna Shale of late Paleocene–early Eocene age, and the overhanging Theban Limestone of early Eocene age (Said 1990) [Fig. 2:C].

The Tarawan Chalk Formation represents the oldest rock unit in the area and is exposed in some localities, and as a sub-surface unit at the Temple entrance. It consists of soft, white, fine-grained chalk and chalky limestone. It can also be observed in excavations in the el-Asasif area (Dupuis et al. 2011).

The Esna Shale Formation overlies the Tarawan Chalk and outcrops broadly and continuously at the foot of the frontal cliff, forming the plain of el-Asasif and the floor of the natural circus of Deir el-Bahari. The formation is a heterogeneous succession (up to 60 m thick) of whitish-grey and greenish shales with gypsum streaks, intercalated with marl near its top. The contact plane with the overlying Theban

Limestone Formation is generally gradational; it is remarkably well exposed in the rocky bay of Deir el-Bahari.

The Theban Limestone Formation (~48 million years; Said 1990) consists mainly of a succession of massive limestone beds with cherty concretions and minor marl beds. King et al. (2017) divided the Theban Limestone Formation exposed in the area of the west bank (up to 340 m thick) into five prominent, cliff-forming, limestone units. The present study is concerned with the lower part of the Theban Limestone rocks, corresponding to King's cliffs 1 and 2 directly overlying the Esna Shale.

These rock units are unconformably overlain by Quaternary alluvial fan-glomerate deposits (sandy gravel interbeds with mudstones) of Pleistocene age (~2.5 million years; Said 1990). These deposits occur on the northeastern side of the Hatshepsut Temple as well as at the western edge of the hills of Sheikh Abd el-Qurna and el-Khokha.

GEOLOGICAL STRUCTURAL FEATURES

The study area is located along the southwestern side of the Qena bend of the Nile Valley. It is generally covered with sedimentary rocks which are distinguished by gentle dips ranging between about 10° – 15° , the values increasing near the ranges of the faults up to 250° . Faults and fractures are the predominant structural features affecting the area. During the Oligocene–Miocene periods, most of these faults and joints (fractures) are believed to have rejuvenated in relation with the Red Sea and Nile Valley tectonics (Said 1990). The main structural trends recorded in the studied area are

N–S, E–W, N35°–45°W, N20°–25°E, and N45°E. They are mainly related to those previously mentioned by El Younsy et al.

(2009) that generally strike ENE–WSW and NE–SW together with the N–S fault trends [Fig. 3:A–D].

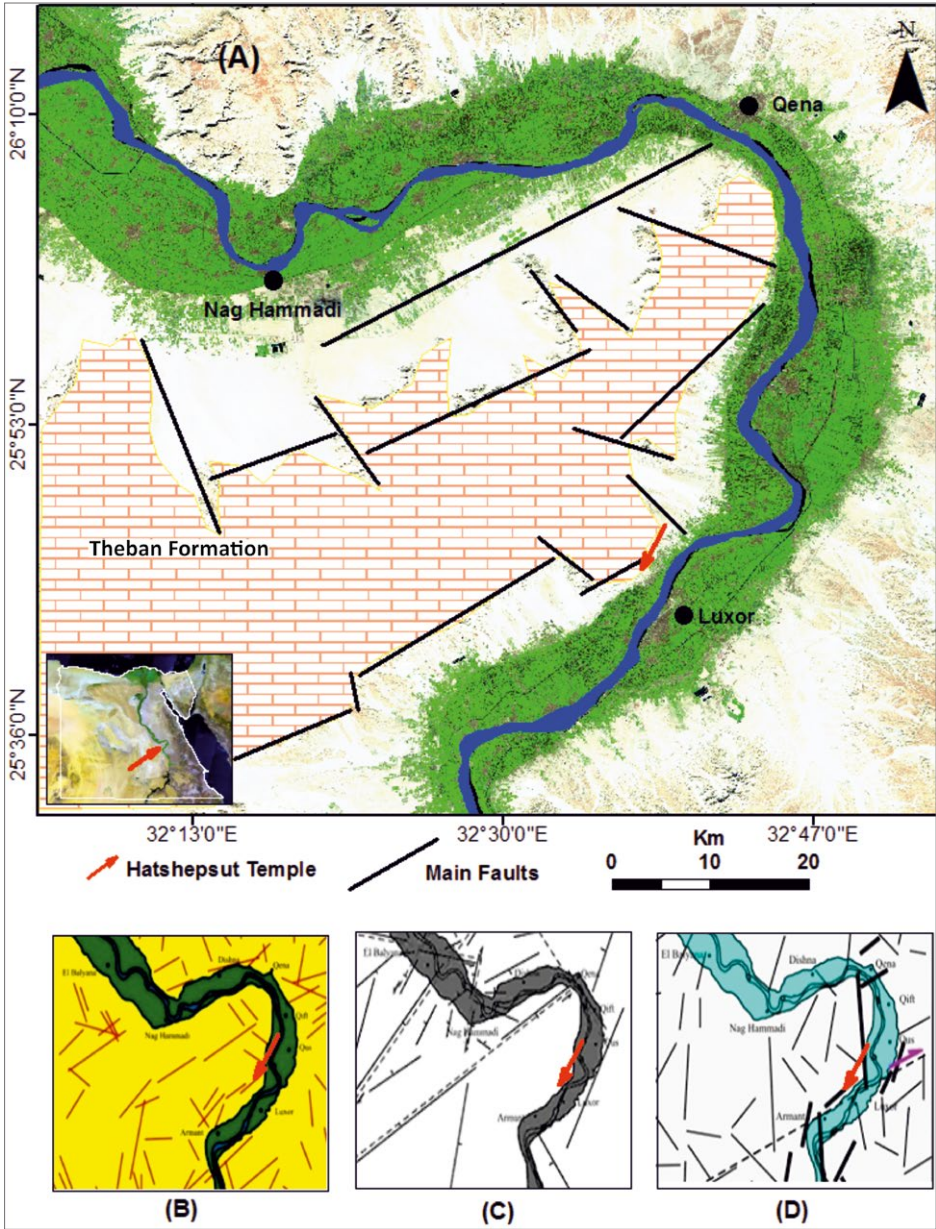


Fig. 3. Geological structural features: A – map tracing the main fault trends in the study area; B, C, D – major faults and fractures deduced from surface, gravity, and aeromagnetic data (© Authors, after El Younsy et al. 2009)

RESULTS AND DISCUSSIONS

GEOLOGICAL ANALYSIS

Recognizing the geological structural framework is a vital first step in understanding and evaluating the state of the cliff above Deir el-Bahari. Thus, to enhance and understand the tectonic effect, as well as the geological setting and potential causes of cliff instability, a detailed structural analysis was done in 31 observation stations. More than 330 faults and/or joints were detected and measured [Figs 4, 5]. These fractures are generally characterized by a vertical dip angle (85° to 90°) and a few sets with the dip angle ranging between 25° and 55° . About 130 fractures, located between the bigger faults and joints in the northeast-

ern sector of the Temple, were measured and found to present varied directions of E-W, $N30^{\circ}$ – 35° W, $N28^{\circ}$ E, $N45^{\circ}$ W, and $N80^{\circ}$ W. About 50 fractures were recorded southwest of the Hatshepsut temple (above the structures of Thutmose III and Mentuhotep II) with the dominant trends there being N–S, E–W, $N35^{\circ}$ – 45° W, $N20^{\circ}$ – 25° E, and $N45^{\circ}$ E. Dense sets of faults and joints (about 150 measurements) were detected in the Theban Limestone cliff above the Temple, with most of them dying out downward in the Esna Shale with noticeable changes in their dip angles. They varied in their directions between N–S, E–W, $N35^{\circ}$ – 40° E, $N20^{\circ}$ – 25° E, and $N65^{\circ}$ W. The main trend in the Theban



Fig. 4. General view of the dense fracturing of the cliff above the Temple (© Authors)

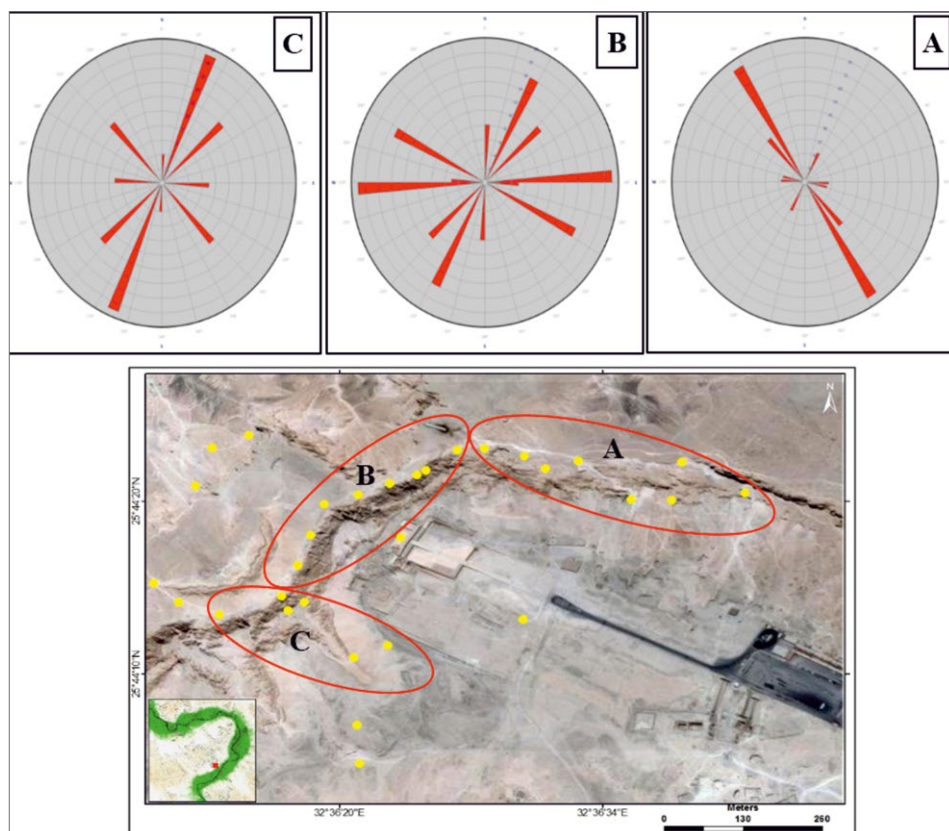


Fig. 5. Rose diagram of detected faults and joints: A – northeastern sector; B – cliff above the Temple; C – sector southwest of the Temple (the locations marked in the picture below) (© Authors)



Fig. 6. The cliff around the bay of Deir el-Bahari: the marks reveal the nearly E-W trend parallel to the temple axis and the N25°E faults (© Authors)



Fig. 7. Intersections between E-W and N25°E faults, causing hanging blocks, big open fractures and unstable isolated blocks above the Temple (© Authors)

cliff above the Temple is a major N20°–25°E fault.

The intersection of the major fault trends (E–W, N30°W, and N25°E) affecting the area [Fig. 6] led to the development of about 18 hanging limestone blocks on the cliff above the Temple, forming separated chimneys (1 to 2 m wide) that could threaten the Temple site in conse-

quence of successive erosional and weathering action in the future [Fig. 7]. Two conjugate systems of joints (N30°W and N25°E) have been noted all over the site, cutting through the big, hanging rock masses. In many localities, the separation of these limestone blocks decreases downwards up to 20-to-50 cm, forming a V-shape [Fig. 8] filled with different-size

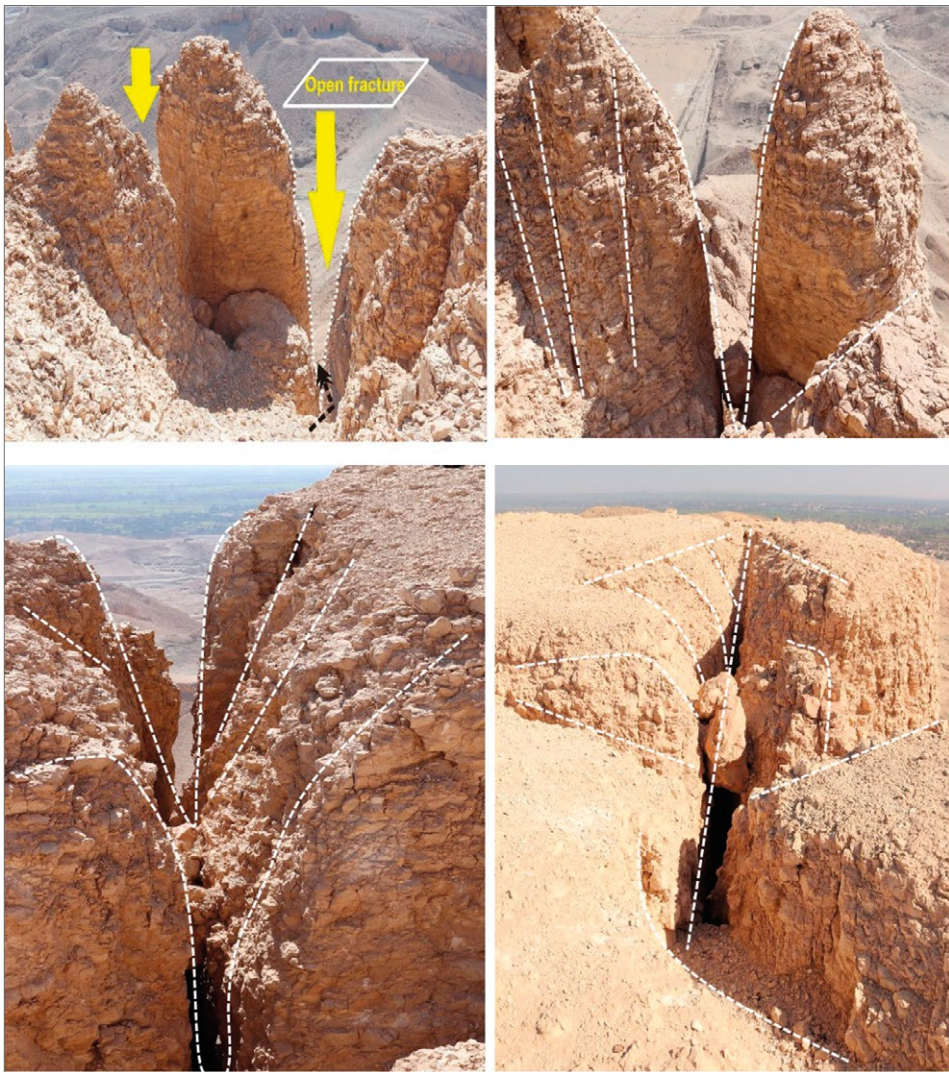


Fig. 8. Separated masses of limestone with V-shaped horizontal displacement (© Authors)

rock fragments at the top and padded with gypsum and calcite mineralization in the lower parts above the Esna Shale. The lack of mineralization along these joints at the top of the limestone hanging blocks implies that the joints could still be active under certain conditions, such as during heavily wet periods.

Generally, the growth and formation of these faults and joints proves that they were formed after the deposition of the Lower Eocene Theban Limestone, as a result of major tectonic events, and therefore they are more recent than the Limestone. Also, these faults and joints did not affect the Quaternary rocks (~2.5 million years) unconformably overlying them, indicating that they are older. This leaves no doubt that these faults are much older than the ancient buildings in the area. However, the exact age of these faults and joints cannot be determined. These faults and joints are currently inactive;

therefore, they are rather not expected to have a destructive impact. However, they could facilitate the action of other potentially high-risk factors.

LABORATORY ANALYSES

The Esna Shale layer, into which the Temple is cut, could be characterized as having a swelling nature due to the availability of flood water and other resources (e.g., groundwater upward seepage), which is reflected in the structure of the site. Therefore, the shales were sampled in order to determine their rock and mineral characteristic, and to estimate the clay mineral content.

X-ray diffraction analysis of the clay-size fraction (<2 μm) of selected samples showed a different composition of both clay and non-clay minerals. Clay minerals (the main target) are composed of predominantly smectite, smectite/illite mixed layer, illite, sepiolite, palygorskite,

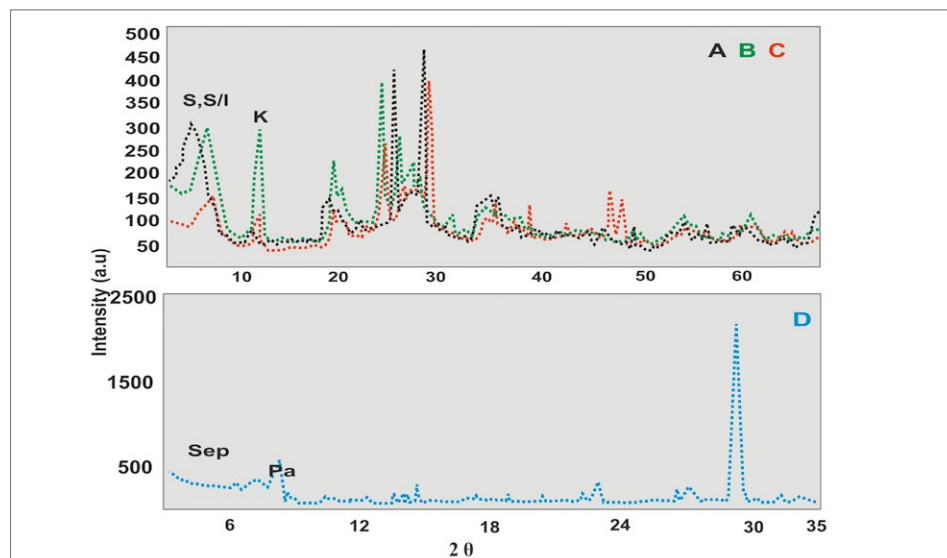


Fig. 9. XRD analysis of Esna Shale (A, B, C) and Theban Limestone (D): S=smectite; S/I=mixed-layer smectit/illite, K=kaolinite, Sep=sepiolite, Pa=palygorskite (© Authors)

and kaolinite. The Esna Shale samples are characterized by the presence of smectite (about 22.5%), illite (about 8.1%), smectite/illite mixed layer (about 10.1%), and kaolinite (about 5.6%) [Fig. 9:A–D]. Abundant smectite and smectite/illite mixed layers are the principal factors behind the expandability of Esna Shale (Abou El-Anwar, EL-Wekeil, and Gaafar 2013).

Esna Shale contains many clay minerals characterized by free-swelling and contraction, which causes the movement of the overlying rocky masses, sometimes leading to catastrophic results. Therefore, samples of Esna Shale were subjected to a free-swelling test. The free-swelling values of the analyzed samples ranged between 8.5% and 10.2%, which is classified as a high swelling rate (Seed, Woodward, and Lundgren 1962). The results match values proposed by Saad A. Aiban (2006).

The Theban Limestone samples contain about 11.2% smectite, 9.8% sepiolite,

and 10.1% palygorskite. This suggests that environmental fluctuations could cause the rock to expand perpendicular to the bedding planes.

ENVIRONMENTAL FACTORS

Environmental factors affecting the area include natural climate influence and seismicity, as well as anthropogenic activity.

Climate

The climate of the Luxor region from 5000 BP until today has been drying successively, with several wetter episodes along the way (Zachos et al. 2001). The climatic data for the Deir el-Bahari region was collected for an interval between 1943 and 2020, showing the impact of climatic variability over 78 years. The intensity of such variability is likely to increase with the global warming, resulting in an increase in rainstorm intensity and consequently enhanced rock falls.

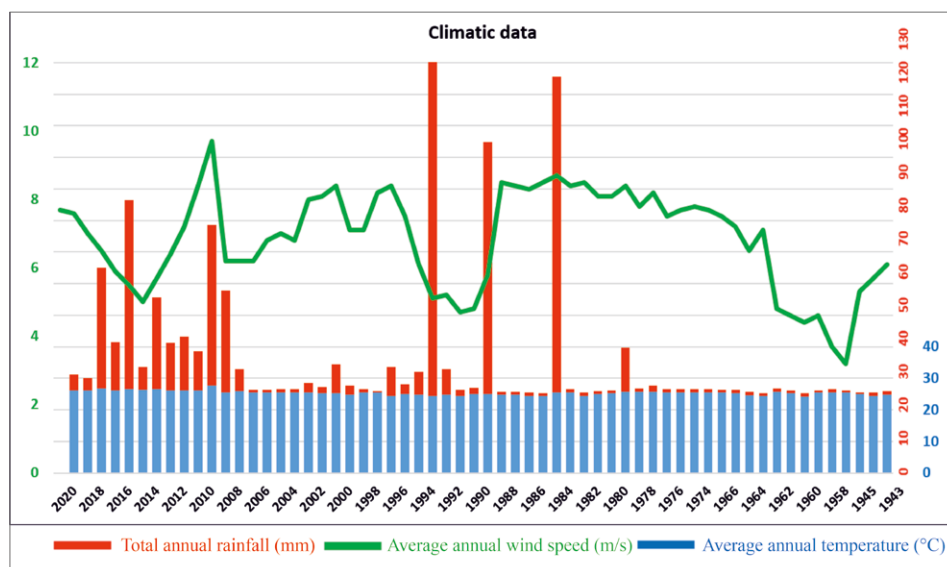


Fig. 10. Climatic data from the area around Luxor showing the parameters for the interval between 1943 and 2020 (© Authors)

The growing precipitation in the Deir el-Bahari area is the cause of an increased frequency of flash floods. For example, in 1994, a destructive flash flood in Upper Egypt (Deir el-Bahari, Luxor) reached maximum values of up to 123.7 mm (Strudwick 1995; Brock 1996). The precipitation variability chart shows periods of increase and decrease in rainfall [Fig. 10]. A marked decrease in rainfall (1.5 mm) is observed between 1943 and 1984, followed by a significant increase in rainfall (31.97 mm) between 1985 and 1994, with another significant decrease (12.89 mm) between 1995 and 2020.

Many karst features are the result of frequent dissolution and erosion caused by rain-related weathering in the past. Fracture systems of different directions have also promoted these effects. Water leaching and filtration through the joints and fractures contributed to the free-swelling of the clay rocks below.

Temperature and wind speed variations could have significant impact on

near-surface conditions through mechanical weathering, causing the rock masses to be stressed and to deteriorate over time. Mean temperatures demonstrate a continuously growing trend: 1.0°C in the period in question, from 32.8°C to 33.8°C between 1943 and 2020. The annual mean of the minimum and maximum temperatures for Deir el-Bahari fluctuates between about 14.9°C and 35.7°C. Also, the average annual wind speed for the period between 1943 and 2020 is about 6.85 m/s. The maximum value is 9.7 m/s in 1965, the minimum value 3.2 m/s in 2017.

Seismicity hazards

The historical earthquake information is an important factor in defining the level of seismicity and determining its future recurrence. Between 2200 BCE and 1899 CE, 83 earthquakes have been recorded in Egypt based on Arabic sources and manuscripts (Badawy 1999). The region around Luxor is generally one of low

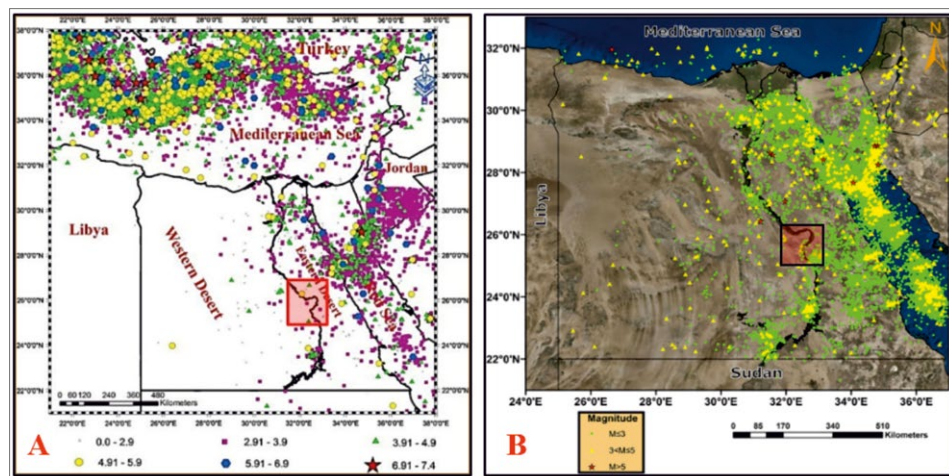


Fig. 11. Seismicity maps (area of Deir el-Bahari in box): A – seismicity magnitude map of Egypt and the Mediterranean (After Mohamed et al. 2012); B – induced seismicity map of Egypt (quarry blasts) (After Badawy et al. 2019)

seismicity, with only a few earthquakes (2–4) recorded in the 20th century. The earliest probable earthquake dates from 600 BCE in Thebes. A high-intensity quake in 967 CE damaged a wall in the Karnak Temple. In 997, 30 years later, a strong earthquake was reported at Qus, a city about 30 km north of Luxor (Karakhanyan, Avagyan, and Sourouzian 2010). A recent seismicity map of Egypt

shows the Luxor area in a zone of moderate seismicity magnitudes (Mohamed et al. 2012) [Fig. 11:A]. Seismic activity does not necessarily trigger failures, but repeated earthquakes are likely to weaken the rock masses in the area. Other sources of seismicity include manmade threats, such as quarry blasts, which create a seismic micro-zonation hazard zone with 3–5 magnitude (Badawy et al. 2019) [Fig. 11:B].

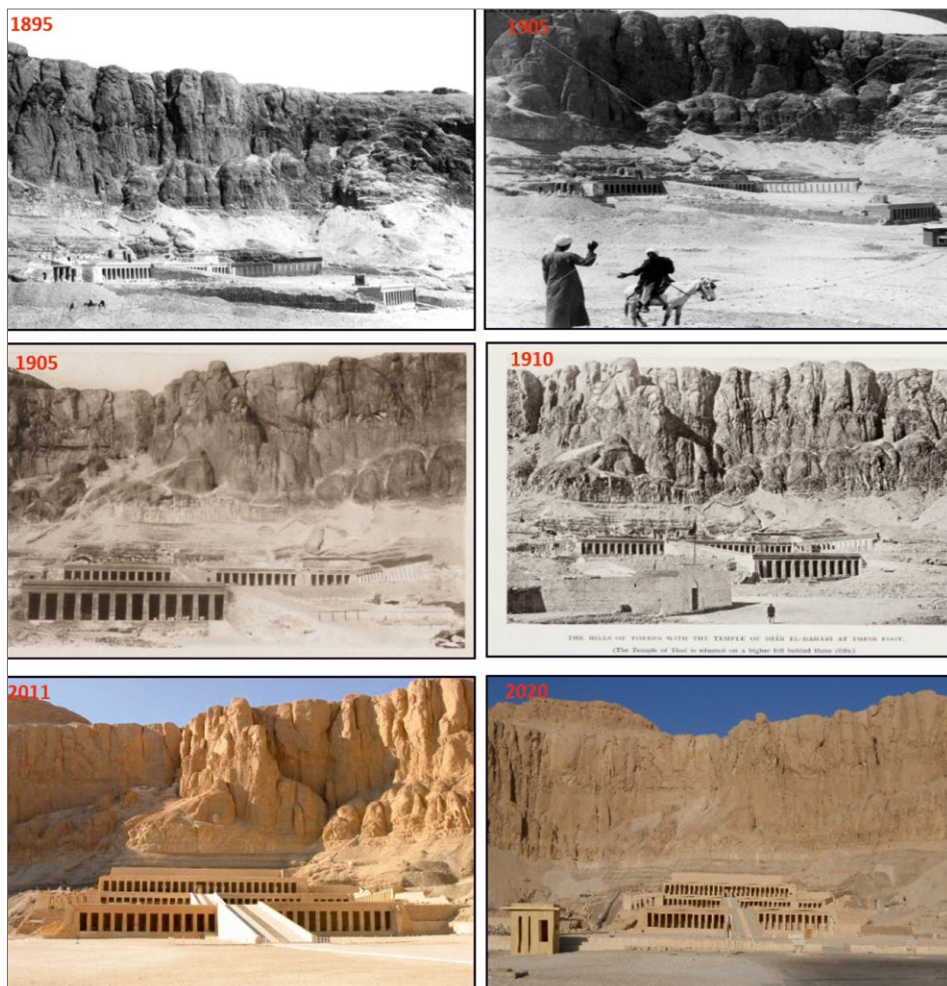


Fig. 12. An example of temporal changes to the rock cliff and hanging blocks above the Temple: stereograph (Images 1895, 1905, 1910: GRANGER and Library of Congress; 2011 and 2020: Authors; stereo © Underwood & Underwood)

PHOTOGRAPHIC DOCUMENTATION

The photographic documentation is an essential visual tool for long-term monitoring of the exposed hanging-rock masses above the Temple. This represents an accurate evaluation of the potential for cliff fracturing and instability of the rock masses. One advantage of this tool is the use of a high precision photogrammetric technique to present an updated record of changes observed in detailed historical documentation and to predict the situation of the hanging blocks and cliff stability in the future. Moreover, the photographic documentation allows the tracts (trajectories) of the falling blocks or boulders to be predicted. In the examples presented here, the visual contrast of photographs of the hanging-rock masses above the Temple from the period between 1895 and 2020 reveals that the cliff is mostly stable except for a few small fragments and exfoliation [Fig. 12]. Some limestone debris that could constitute a hazard was detected.

HYPOTHETICAL IMPACT MODEL

The discussion presented here served as the groundwork for developing a hypothetical impact model showing the probability of past, present and future scenarios of environmental and swelling threats endangering the temple site [Fig. 13]. Thus, water infiltrating through the fractured Theban Limestone during occasional rainfall, flooding, and then uneven drying up events, causes the swelling of the underlying Esna Shale, which, in the long run, weakens the rock masses forming the cliff above the Temple.

The contact zone between the Esna Shale and the overlying limestone cliff behind the Temple is generally sharp, especially in the area of the archaeological site, but close observation of the expected undulations over a large area requires more unrestricted field investigations to confirm the nature and current condition of the contact zone between the different rock units.

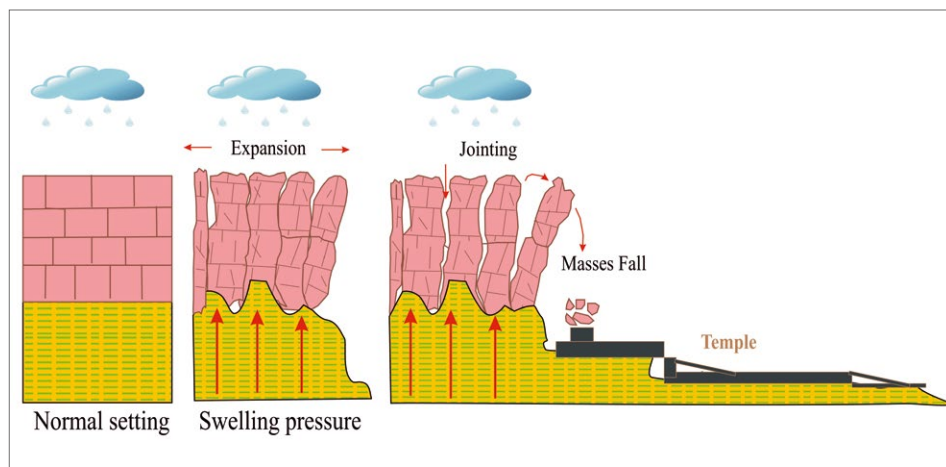


Fig. 13. A 2D hypothetical impact model illustrating the temporal changes of the cliff above the Temple site (© Authors)

CONCLUSIONS AND RECOMMENDATIONS

To conclude, the impact of the geological analysis of the Deir el-Bahari area cannot be overestimated indeed, as it provides data indispensable for a qualitative and scientific assessment of potential threats to the historical monuments. The investigations so far revealed the following:

- Sets of faults and joints affect the Theban Cliff and threaten the Temple. A noticeable horizontal separation of the limestone rock masses ranged in width from 1 m to 2 m at the top, forming a V-shape that decreased downwards from 0.20 m to 0.50 m. Trends were recorded along some of the E–W, N30°W, and N25°E lines. Successive erosion and weathering could be the cause of the displacement of these masses.
- Although the exact age of these faults and joints is difficult to determine, still they may be younger than the Theban limestone unit and much older than the Quaternary rocks (about

2.5 million years) and consequently also the ancient buildings in the area.

- About 18 hanging blocks and pillars (mainly isolated) were recorded. These could pose a hazard. Otherwise, there is no indication of a precise time for recent horizontal or vertical displacement of these hanging blocks.
- Small fragments and exfoliation, as well as limestone debris, were recorded scattered along the face of the limestone cliff and in between some of the pillars. These could be a lesser risk.

After monitoring all of the factors posing a threat to the limestone cliffs above the Temple, it has to be said that they continue to be dangerous. In order to propose effective solutions for the protection of the Temple, a detailed mapping of the area is essential to integrate the geological and environmental impact data, as well as to prepare a database for long-term static and dynamic monitoring of the separated blocks one by one.

Dr. Patryk Chudzik

<https://orcid.org/0000-0003-3882-8797>
University of Warsaw, Polish Centre
of Mediterranean Archaeology
pm.chudzik@uw.edu.pl

Prof. Ahmed-Reda M. El Younsy

<https://orcid.org/0000-0003-1162-0435>
University of Assiut, Faculty of Science,
Geology Department
Assiut, Egypt
elyousny@aun.edu.eg

How to cite this article: Chudzik, P., El Younsy, A.R.M., Galal, W.F., and Salman, A.M. (2021). Geological appraisal of the Theban cliff overhanging the Hatshepsut temple at Deir el-Bahari. In P. Chudzik and Z.E. Szafranski (eds), *Deir el-Bahari Studies 3 (=Polish Archaeology in the Mediterranean 30/1)* (pp. 275–295). Warsaw: WUW <https://doi.org/10.31338/uw.2083-537X.pam30.1.02>

Wael F. Galal

<https://orcid.org/0000-0002-9280-7455>

University of Assiut, Faculty of Science, Geology Department

Asyut, Egypt

waelfathi70@hotmail.com

Dr. Abdelhamid M. Salman

<https://orcid.org/0000-0003-1843-2509>

University of Assiut, Faculty of Science, Geology Department

Asyut, Egypt

salman@aun.edu.eg

References

- Abou El-Anwar, E.A., EL-Wekeil, S.S., and Gaafar, S.S. (2013). Contribution to the mineralogy, geochemistry, and provenance of the Lower Eocene Esna Shale in the Farafra Oasis, Western Desert, Egypt. *Journal of Applied Sciences Research*, 9(8), 5344–5369
- Aiban, S.A. (2006). Compressibility and swelling characteristics of Al-Khobar Palygorskite, eastern Saudi Arabia. *Engineering Geology*, 87(3), 205–219
- Alaska Satellite Facility. (2015). ASF radiometric terrain corrected products. Algorithm Theoretical Basis Document. Retrieved from https://asf.alaska.edu/wp-content/uploads/2019/03/rtc_atbd_v1.2_final.pdf (accessed: 11.09.2021)
- Arnold, D. (1979). *The Temple of Mentuhotep at Deir el Bahari*. New York: Metropolitan Museum of Art
- Arnold, D. (2005). The Temple of Hatshepsut at Deir el-Bahri. In C.H. Roehrig, R. Dreyfus, and C.A. Keller (eds), *Hatshepsut, from queen to Pharaoh* (pp. 135–140). New York: The Metropolitan Museum of Art
- Badawy, A. (1999). Historical seismicity of Egypt. *Acta Geodaetica et Geophysica Hungarica*, 34(1–2), 119–135
- Badawy, A., Gamal, M., Farid, W., and Soliman, M.S. (2019). Decontamination of earthquake catalog from quarry blast events in northern Egypt. *Journal of Seismology*, 23(6), 1357–1372
- Bernhauer, E. (1998). Hathor “an der Spitze von Theben” und ihre Tempelarchitektur. *Göttinger Miszellen*, 164, 15–20
- Brock, L.P. (1996). The Theban flood of 1994. Ancient antecedents and the case of KV 55. *Varia Aegyptiaca*, 11, 1–16
- Ćwiek, A. (2014). Old and Middle Kingdom tradition in the Temple of Hatshepsut at Deir el-Bahari. *Études et Travaux*, 27, 61–93
- Ćwiek, A. (2020). The pyramid of the Theban mountain. In M. Bárta and J. Janák (eds), *Profane landscapes, sacred spaces* (pp. 18–32). Sheffield–Bristol, CT: Equinox
- Dodson, A. (1989–1990). Amenhotep I and Deir el-Bahari. *Journal of the Ancient Chronology Forum*, 3, 42–44

- Dupuis, C., Aubry, M.-P., King, C., Knox, R.W.O., Berggren, W.A., Youssef, M., Galal, W.F., and Roche, M. (2011). Genesis and geometry of tilted blocks in the Theban Hills, near Luxor (Upper Egypt). *Journal of African Earth Sciences*, 61(3), 245–267
- Eigner, D. (1984). *Die monumentalen Grabbauten der Spätzeit in der thebanischen Nekropole* (=Denkschriften der Gesamtakademie 8). Vienna: Verlag der Österreichischen Akademie der Wissenschaften
- Ejsmond, W. (2018). Natural pyramids of Ancient Egypt: From emulations of monarchs to royal burials. *Ägypten & Levante*, 28, 169–180
- El Younsy, A.R.M., Ibrahim, H.A., Senosy, M.M., and Galal, W.F. (2009). Structural characteristics and tectonic evolution of the area around the Qena bend, Middle Egypt. In *The Sixth International Conference on the Geology of Africa* (pp. IV-1–23). Assiut
- Geological map of Egypt*. (1986–1987). Cairo: Conoco; Egyptian General Petroleum Corporation
- Godlewski, W. (1986). *Le monastère de St Phoibammon* (=Deir el-Bahari 5). Warsaw: PWN – Éditions Scientifiques de Pologne
- Karakhanyan, A., Avagyan, A., and Sourouzhian, H. (2010). Archaeoseismological studies at the temple of Amenhotep III, Luxor, Egypt. In M. Sintubin, I.S. Stewart, T.M. Niemi, and E. Altunel (eds), *Ancient earthquakes* (=Geological Society of America Special Papers 471) (pp. 199–222). Boulder, CO: Geological Society of America
- King, C., Dupuis, C., Aubry, M.-P., Berggren, W.A., Knox, R.O.B., Galal, W.F., and Baele, J.-M. (2017). Anatomy of a mountain: The Thebes Limestone Formation (Lower Eocene) at Gebel Gurnah, Luxor, Nile Valley, Upper Egypt. *Journal of African Earth Sciences*, 136, 61–108
- Lipińska, J. (1977). *The temple of Tuthmosis III. Architecture* (=Deir el-Bahari 2). Warsaw: PWN – Éditions Scientifiques de Pologne
- Lipińska, J. (2005). The Temple of Tuthmosis III at Deir el-Bahari. In C.H. Roehrig, R. Dreyfus, and C.A. Keller (eds), *Hatshepsut, from queen to Pharaoh* (pp. 285–288). New York: The Metropolitan Museum of Art
- Madej, A. (2018). Stamped bricks of Amenhotep I from Deir el-Bahari. In Z.E. Szafrński (ed.), *Deir el-Bahari studies 2* (=Polish Archaeology in the Mediterranean 27/2) (pp. 291–300). Warsaw: University of Warsaw Press
- Mohamed, A.E.-E.A., El-Hadidy, M., Deif, A., and Abou Elenean, K. (2012). Seismic hazard studies in Egypt. *NRIAG Journal of Astronomy and Geophysics*, 1(2), 119–140
- Niwiński, A. (2008). Mein Gesicht ist auf Amun gerichtet: ein Vorschlag der Identifizierung einer Kultstätte in Theben-West. *Göttinger Miszellen*, 217, 7–8
- Said, R. (1990). *The geology of Egypt*. Rotterdam: Balkema
- Seed, H.B., Woodward, R.J., and Lundgren, R. (1962). Prediction of swelling potential for compacted clays. *Journal of the Soil Mechanics and Foundations Division*, 88(3), 53–87
- Smilgin, A. (2012). Sandstone sphinxes of Queen Hatshepsut from Deir el-Bahari: Preliminary remarks. *Polish Archaeology in the Mediterranean*, 21, 255–260

- Strudwick, N. (1995). Flood damage in Thebes. *Biblical Archaeology*, 58, 116–117
- Winlock, H.E. (1924). The Egyptian Expedition, 1923–1924. *Bulletin of the Metropolitan Museum of Art*, 19(2), 5–33
- Winlock, H.E. (1928a). The Egyptian Expedition 1925–1927: The Museum's excavations at Thebes. *Bulletin of the Metropolitan Museum of Art*, 23(2), 3–58
- Winlock, H.E. (1928b). The Egyptian Expedition 1927–1928: The Museum's excavations at Thebes. *Bulletin of the Metropolitan Museum of Art*, 23(12), 3–28
- Winlock, H.E. (1932). The Egyptian Expedition 1930–1931: The Museum's excavations at Thebes. *Bulletin of the Metropolitan Museum of Art*, 27(3/2), 4–37
- Zachos, J., Pagani, M., Sloan, L., Thomas, E., and Billups, K. (2001). Trends, rhythms, and aberrations in global climate 65 Ma to present. *Science*, 292(5517), 686–693

Websites

- <http://eros.usgs.gov>
<http://climatetoolbox.org>
<http://climatologylab.org>

